



HAL
open science

An optimally tuned range-separated hybrid starting point for ab initio GW plus Bethe-Salpeter equation calculations of molecules

Caroline Mckeon, Samia Hamed, Fabien Bruneval, Jeffrey Neaton

► **To cite this version:**

Caroline Mckeon, Samia Hamed, Fabien Bruneval, Jeffrey Neaton. An optimally tuned range-separated hybrid starting point for ab initio GW plus Bethe-Salpeter equation calculations of molecules. *The Journal of Chemical Physics*, 2022, 157, pp.074103. 10.1063/5.0097582. cea-04176651

HAL Id: cea-04176651

<https://cea.hal.science/cea-04176651>

Submitted on 3 Aug 2023

HAL is a multi-disciplinary open access archive for the deposit and dissemination of scientific research documents, whether they are published or not. The documents may come from teaching and research institutions in France or abroad, or from public or private research centers.

L'archive ouverte pluridisciplinaire **HAL**, est destinée au dépôt et à la diffusion de documents scientifiques de niveau recherche, publiés ou non, émanant des établissements d'enseignement et de recherche français ou étrangers, des laboratoires publics ou privés.

An optimally tuned range-separated hybrid starting point for *ab initio* GW plus Bethe–Salpeter equation calculations of molecules

EP

Cite as: J. Chem. Phys. **157**, 074103 (2022); <https://doi.org/10.1063/5.0097582>

Submitted: 29 April 2022 • Accepted: 08 July 2022 • Published Online: 17 August 2022

 Caroline A. McKeon, Samia M. Hamed,  Fabien Bruneval, et al.

COLLECTIONS

 This paper was selected as an Editor's Pick



View Online



Export Citation



CrossMark

ARTICLES YOU MAY BE INTERESTED IN

Density-functional theory vs density-functional fits

The Journal of Chemical Physics **156**, 214101 (2022); <https://doi.org/10.1063/5.0091198>

Impact of the current density on paramagnetic NMR properties

The Journal of Chemical Physics **157**, 031102 (2022); <https://doi.org/10.1063/5.0103898>

Software for the frontiers of quantum chemistry: An overview of developments in the Q-Chem 5 package

The Journal of Chemical Physics **155**, 084801 (2021); <https://doi.org/10.1063/5.0055522>

Lock-in Amplifiers
up to 600 MHz



Zurich
Instruments



An optimally tuned range-separated hybrid starting point for *ab initio* GW plus Bethe–Salpeter equation calculations of molecules

Cite as: J. Chem. Phys. 157, 074103 (2022); doi: 10.1063/5.0097582

Submitted: 29 April 2022 • Accepted: 8 July 2022 •

Published Online: 17 August 2022



View Online



Export Citation



CrossMark

Caroline A. McKeon,^{1,2,3}  Samia M. Hamed,^{1,2,3,a)} Fabien Bruneval,⁴  and Jeffrey B. Neaton^{1,2,3,5,b)} 

AFFILIATIONS

¹ Department of Physics, University of California, Berkeley, California 94720, USA

² Department of Chemistry, University of California, Berkeley, California 94720, USA

³ Natural Sciences Division, Lawrence Berkeley National Laboratory, Berkeley, California 94720, USA

⁴ Université Paris-Saclay, CEA, Service de Recherches de Métallurgie Physique, 91191 Gif-sur-Yvette, France

⁵ Kavli ENSI, University of California, Berkeley, California 94720, USA

^{a)} Current address: Intel Corporation, Santa Clara, CA 95054.

^{b)} Author to whom correspondence should be addressed: jbneaton@lbl.gov

ABSTRACT

The *ab initio* GW plus Bethe–Salpeter equation (GW-BSE, where G is the one particle Green’s function and W is the screened Coulomb interaction) approach has emerged as a leading method for predicting excitations in both solids and molecules with a predictive power contingent upon several factors. Among these factors are the (1) generalized Kohn–Sham eigensystem used to construct the GW self-energy and to solve the BSE and (2) the efficacy and suitability of the Tamm–Dancoff approximation. Here, we present a detailed benchmark study of low-lying singlet excitations from a generalized Kohn–Sham (gKS) starting point based on an optimally tuned range-separated hybrid (OTRSH) functional. We show that the use of this gKS starting point with one-shot G_0W_0 and G_0W_0 -BSE leads to the lowest mean absolute errors (MAEs) and mean signed errors (MSEs), with respect to high-accuracy reference values, demonstrated in the literature thus far for the ionization potentials of the GW100 benchmark set and for low-lying neutral excitations of Thiel’s set molecules in the gas phase, without the need for self-consistency. The MSEs and MAEs of one-shot G_0W_0 -BSE@OTRSH excitation energies are comparable to or lower than those obtained with other functional starting points *after* self-consistency. Additionally, we compare these results with linear-response time-dependent density functional theory (TDDFT) calculations and find GW-BSE to be superior to TDDFT when calculations are based on the same exchange–correlation functional. This work demonstrates tuned range-separated hybrids used in combination with GW and GW-BSE can greatly suppress starting point dependence for molecules, leading to accuracy similar to that for higher-order wavefunction-based theories for molecules without the need for costlier iterations to self-consistency.

Published under an exclusive license by AIP Publishing. <https://doi.org/10.1063/5.0097582>

I. INTRODUCTION

Electronic excitations in organic molecules are central to diverse areas of study, including the development of clean energy technologies, such as organic electrodes in batteries,¹ dye-sensitized solar cells,² and photocatalysis in light-harvesting nanomaterials.³ Decades of work have resulted in an increasingly large tool-set of single- and multireference wavefunction-based computational

methods and a concomitant ever-expanding library of detailed benchmark studies.^{4–13} These studies report on the accuracy of methods for predicting singlet and triplet excited states, low- and high-lying singly and multiply excited states that are local, extended, charge-transfer, or Rydberg in small- and medium-sized molecules.

In parallel to advances in wavefunction-based methods, the linear-response time-dependent density functional theory

(TDDFT)^{14–18} approach within adiabatic approximations remains the most popular excited state method in use today for neutral excitations in molecules. It is efficient and versatile, with a formal $\mathcal{O}(N^3)$ or $\mathcal{O}(N^2)$ scaling with system size,¹⁹ the ability to couple to environmental models^{20,21} to produce excited state potential energy surfaces, and to treat spin-relativistic effects,²² all with average excitation energy errors approaching 0.2 eV.²³ However, the good general performance of TDDFT is not unqualified and its limitations, such as inaccurate description of charge-transfer states, are well documented in the literature.^{24–27} Additionally, while the inclusion of asymptotic long-range exact exchange in hybrid functionals is well known to improve the singlet energies,²⁸ it can lead to significant underestimations of triplet energies, resulting in improper state ordering or triplet instabilities,²⁹ a deficiency that can be partially remedied by the Tamm–Dancoff approximation (TDA).³⁰

In recent years, the *ab initio* GW plus Bethe–Salpeter equation (GW-BSE) approach based on many-body perturbation theory (MBPT)^{13–33,42,44,98} formalism has emerged as a method that can be accurate and efficient for charged excitations while possessing similar or greater accuracy relative to TDDFT for neutral excitations of molecules.^{34–40} In the GW-BSE approach, charged and neutral excitations are computed by solving approximate solutions to Dyson-like equation for the one- and two-particle many-body Green’s functions, respectively. The self-energies appearing in these equations are truncated at low orders of perturbation theory and constructed in a multistep process. First, the GW self-energy, $\Sigma = iGW$, the result of a diagrammatic expansion in Σ to lowest order in W , is constructed by convolving the single-particle Green’s function, G , with the frequency-dependent, screened Coulomb interaction W . In practice, both G and W are built with states and energies taken from a generalized Kohn–Sham (KS) eigensystem, with W constructed within the random-phase approximation (RPA). The gKS eigenvalues are then perturbatively corrected to first order in Σ , leading to a sensitivity of the resultant quasiparticle eigenvalues to the underlying gKS system, a starting point dependence that is sometimes mitigated by iteratively updating Σ .^{41–44} The one-particle states are then coupled in a two-particle BSE via the electron–hole interaction kernel. In this static limit, the BSE is written in a form analogous to TDDFT’s Casida equations, except the BSE is built upon GW-corrected one-particle energies and further, in the BSE, the f_{xc} kernel of the Casida equations is replaced with W (Fig. 1).^{45–47} We then solve the BSE to yield singlet excitations.^{34,41}

As mentioned previously, the GW self-energy can be sensitive to the gKS starting point. While solutions have been proposed to address this starting point dependence, achieving a balance between computational cost and accuracy remains challenging. One example is a consistent starting point scheme in which the best α parameter in a global hybrid is chosen so that the GW correction for the quasiparticle spectrum, not just the highest occupied molecular orbital (HOMO), is minimized via rigid shift of all eigenvalues.^{48–50} Although this consistent starting point method has never been benchmarked for G_0W_0 -BSE neutral excitations, prior work on organic molecules, such as pyridine, benzene, and pentacene, led to $\alpha = 0.25$ – 0.3 .⁴⁸ The global hybrid BHLYP, which has 50% exact exchange, has been reported to perform well as a G_0W_0 -BSE starting point for singlet excitations relative to experiment.^{4,34,50} BHLYP

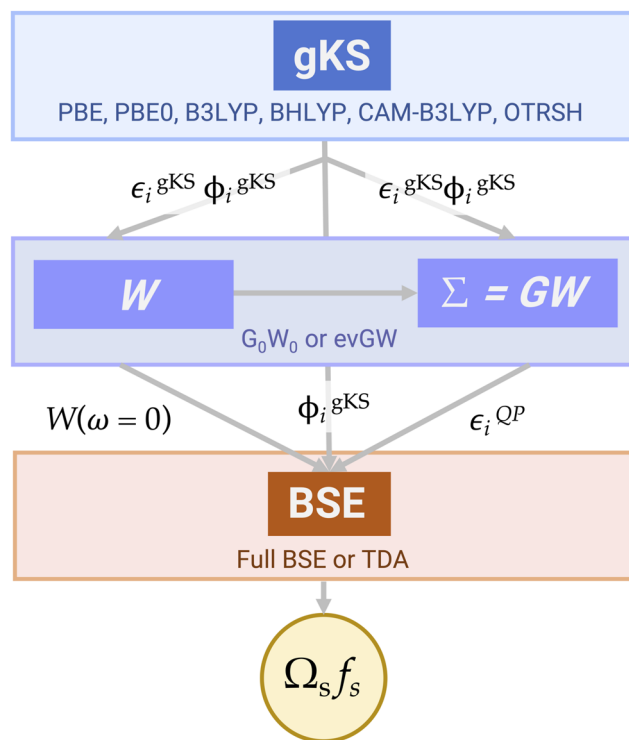


FIG. 1. GW-BSE workflow used in this study with variations in approximations listed in their corresponding box. In the upper box, the outcomes of the generalized Kohn–Sham DFT calculation for each Thiel set molecule with fixed nuclei are the resulting eigenvalues (ϵ_i^{gKS}) and gKS wavefunctions (ϕ_i^{gKS}) of the gKS eigensystem. The GW calculation in the middle box involves the construction of the screened Coulomb interaction (W) and yields quasiparticle energies (ϵ_i^{QP}). These quantities, along with the original gKS wavefunction, are input for the BSE calculation in the bottom box. Finally, the neutral excitation energies (Ω_s) and corresponding electron–hole amplitudes (f_s) are output from the BSE calculation. The schematic is adapted from Bruneval *et al.*, *Comput. Phys. Commun.* **208**, 149 (2016).

does not perform as well for triplet excitations, however. The functionals PBE0 and B3LYP, which have 25% exact exchange (similar to the consistent starting point schemes) are excellent starting points for TDDFT, as is CAM-B3LYP,^{51–53,54} but poor starting points for G_0W_0 -BSE neutral singlet and triplet excitations.

In this work, we focus on the utility of IP-tuned hybrids, e.g., the optimally tuned range-separated hybrid (OTRSH), which yield accurate KS-HOMO energies by design and have shown good agreement with experiment for the whole excitation spectrum for molecular systems.^{55–61} For molecules, the use of optimally tuned range-separated hybrid functionals that enforce the IP theorem as a starting point for G_0W_0 , as suggested by Refaely–Abramson *et al.*,⁵⁵ has been shown to be successful.^{57–60,62,63} Additionally, the use of the OTRSH functional in the GW-BSE framework has also been shown to lead to accurate neutral excitation energies in several cases.⁶² However, a comprehensive benchmark study of GW-BSE@OTRSH for ionization potentials and singlet excitations has yet to be performed against high-accuracy quantum chemistry methods.

In the OTRSH scheme, the Coulomb potential is partitioned into short- and long-range interactions, with different fractions of exact exchange in the short and long range.^{54,64} This partitioning introduces three parameters, α , β , and γ and is expressed as

$$\frac{1}{r_{12}} = \frac{\alpha + \beta \operatorname{erf}(\gamma r_{12})}{r_{12}} + \frac{1 - (\alpha + \beta \operatorname{erf}(\gamma r_{12}))}{r_{12}}. \quad (1)$$

In practice, the first term is retained and the second term is replaced with a semi-local xc functional, such as one of several GGAs. In OTRSH, the range separation parameter, γ , is tuned such that the ionization potential theorem^{65–69} is satisfied, with α fixed to 0.2 and $\alpha + \beta$ set to unity, enforcing that the exchange potential approaches $\frac{1}{r_{12}}$ as r_{12} goes to infinity. Two examples of OTRSH functionals are those of Baer–Neuhauser–Livshitz (BNL),^{70,71} the original OTRSH functional, and the Perdew–Burke–Ernzerhof (PBE)-based OTRSHs.^{55,72,73}

Here, we provide an assessment of the performance of OTRSH as a starting point for G_0W_0 and G_0W_0 -BSE calculations of organic molecules. The OTRSH starting point in combination with the G_0W_0 approach and the TDA has already been shown to yield excellent results for triplets in a subset of 20 molecules in Thiel's set and for the two low-lying difficult-to-simultaneously-capture acene singlets.⁶² We extend this work and evaluate G_0W_0 and G_0W_0 -BSE against multireference and coupled cluster calculations^{74,75} for singlet excitations of organic molecules in Thiel's set. We provide a detailed analysis of the performance of the BSE approach and TDA for this starting point, and compare them with the computationally less expensive TDDFT@OTRSH calculations.

We find that OTRSH is an exceptional starting point for single-shot G_0W_0 and G_0W_0 -BSE, and the use of OTRSH can greatly suppress starting point dependence for neutral excitations of Thiel's set molecules, leading to accuracy similar to that of higher-order wavefunction-based theories at reduced computational cost without the need for several GW-BSE calculations to iterate to self-consistency. The dataset and subsequent analysis presented in this work complement GW-BSE@OTRSH calculations that have already been performed on chromophores and compared to experimental excitation energies.^{76,99}

The structure of this paper is as follows: In Sec. II, we will discuss the benchmark set of molecules and the origins of the best theoretical estimates (BTEs) used in this study and the details of the DFT and GW-BSE calculations performed on these molecules. In Sec. III, we will discuss the performance of G_0W_0 -BSE for the GW100 set with different starting points and various formulations of GW-BSE in predicting singlets. We will then compare the performance of G_0W_0 -BSE to TDDFT in the prediction of singlets in comparison to BTE for these excitations. We will also discuss the performance of G_0W_0 -BSE and evGW-BSE for Thiel's set of organic molecules.

II. METHODS AND COMPUTATIONAL DETAILS

A. Benchmark molecules and their excitations

In this work, we use two well-known sets to explore charged and neutral excitations.

First, the GW100 set⁴⁰ consists of 100 small molecules selected to cover a large variety of chemical bond types and environments. Reference values for the 100 ionization potentials have been obtained through total energy differences with high-level coupled cluster, CCSD(T), by Krause and co-workers.⁷⁷ Recently, these reference values have been updated in Ref. 78, acknowledging the strong dependence of CCSD(T) upon the Hartree–Fock solution.

Then, for neutral excitations, we use Thiel's set of established, high-level quantum chemistry excitation energies of small molecules to benchmark the OTRSH functional as a starting point for GW-BSE calculations. Thiel's benchmark set^{74,75} consists of 103 singlet and 63 triplet excitation energies on 28 small- and medium-sized molecules, including unsaturated aliphatic hydrocarbons, aromatic hydrocarbons and heterocycles, aldehydes, ketones, amides, and nucleobases (Fig. 2).

B. Computational details

Our calculation workflow is illustrated in Fig. 1. The workflow starts with a self-consistent DFT calculation for a molecule with fixed nuclei. Starting from the output of our DFT calculations, and using the MOLGW package,⁴¹ we then construct the GW self-energy and compute one- and two-particle excitation energies with the GW and GW-BSE approaches, respectively. The underlying theory is explained in more detail elsewhere.^{41,44,81,82} As discussed in prior work,^{34,35} GW calculations are sensitive to the generalized Kohn–Sham starting point and to whether self-consistency is used. Here, we evaluate one such starting point, G_0W_0 @OTRSH, against G_0W_0 @B3LYP (single-shot GW on top of B3LYP,⁷⁹ which has 20% exact exchange), G_0W_0 @BHLYP (single-shot GW on top of BHLYP),⁵⁰ G_0W_0 @CAM-B3LYP (single-shot GW on top of CAM-B3LYP)⁵⁴—a range-separated hybrid with 25% short-range exact exchange, and eigenvalue self-consistent GW (evGW)—in which the quasiparticle energies are updated (in both G and the polarizability) one or more times prior to calculating the final self-energy corrections.⁸⁰

These xc functionals are chosen for the following reasons. B3LYP and PBE0 are among the most popular choices for TDDFT calculations, while BHLYP has demonstrated good performance as a starting point for GW-BSE. CAM-B3LYP is an untuned range-separated hybrid that can be compared to OTRSH, and PBE is a representative non-hybrid. With these six functionals, we span the range from 0% to 100% HF exchange in the long range for OTRSH.

In our GW-BSE calculations with the MOLGW package, the frequency dependence of the GW nonlocal self-energy $\Sigma(\mathbf{r}, \mathbf{r}', \omega)$ is treated analytically with the spectral decomposition method; hence, it is exact for a given basis set.⁴¹ We use standard approximations to solve the BSE: Vertex corrections are neglected,^{78,81} the polarizability and other matrix elements are constructed using GW eigenvalues and DFT wavefunctions, the screened Coulomb interaction is evaluated in the random-phase approximation (RPA),⁸² and a static limit is taken for the screened electron–hole interaction kernel.⁴⁵ We use the cc-pVTZ for TDDFT calculations and aug-cc-pVTZ basis sets for GW-BSE calculations⁸³ as employed previously;⁶² the latter ensures convergence better than 0.1 eV for the excitation energies shown here. Following prior work,⁶² we use the resolution-of-identity in the Coulomb metric⁸⁴ as implemented in MOLGW,⁴¹

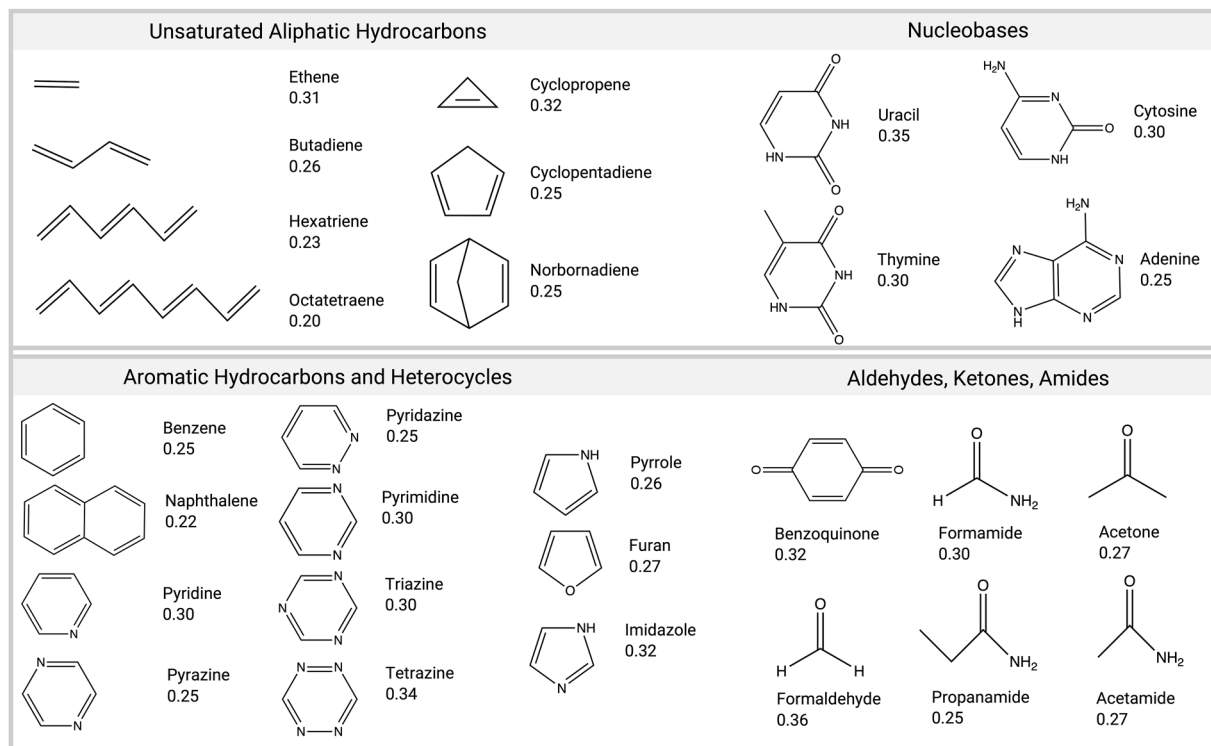


FIG. 2. Molecules from Thiel's set examined in this study, including the optimally tuned range separation parameters (γ) in units of bohr⁻¹ determined in this work.

with the auxiliary basis sets of Weigend,⁸⁵ which are consistent with Dunning basis sets.

We use the MP2/6-31G(d) ground state geometries for Thiel's set,^{74,75} and we have taken BTEs for the singlet and triplet states from Schreiber *et al.*⁷⁴ For GW100, we compare with the CCSD(T) calculations of Bruneval *et al.*⁷⁸ The BTEs for Thiel's set excitations are constructed as follows: Whenever available, highly correlated *ab initio* calculations with large basis sets were used as BTEs; in the absence of such data, coupled cluster response theory methods were used for systems where the ground state is well described by a single determinant and the excited states are dominated by single excitations. CASPT2 was used for multireference systems where the ground state consists of several determinants with large weights. Basis set convergence depended on the nature of the excitations and the methods involved.⁷⁴

The wavefunctions for molecules with inversion symmetry are analyzed for parity via the transition matrix and identified as either *gerade* or *ungerade*. The identification of singlet states is based on parity symmetry, similarity of oscillator strength magnitudes, and overlap of the orbitals involved in the transition with a reference set of orbitals obtained with the G₀W₀-BSE@PBE. Oscillator strength error is reported in the [supplementary material](#). Orbital overlap was determined by calculating the dot product between corresponding wavefunction density entries from volumetric data cube files. We disregarded singlets that were not able to be positively identified for

certain molecules or methods. Excitations and oscillator strengths that are discussed here are listed in the [supplementary material](#).

C. OTRSH

For our OTRSH calculations, we use the range separation form of Eq. (1) and set $\alpha = 0.2$, which leads to $\beta = 0.8$, and fixes the amount of short-range Fock exchange to 20%. Prior works have tuned both α and γ and found limited impact on the optimal α parameter, which remained in the 0.2–0.25 range.^{55,72} This choice for α maintains consistency with other global hybrid functionals and prior work on small gas-phase molecules.^{55,56,86,87} The OTRSH functional used in this work is built with PBE as the underlying GGA contribution.

As in prior work, the range separation parameter γ is varied to enforce the ionization potential theorem of DFT^{65,66,69,88} through minimization of a target function $J^2(\gamma)$,

$$J^2(\gamma) = [\text{IP}^\gamma(N) + \varepsilon_{\text{HOMO}}^\gamma(N)]^2 + [\text{IP}^\gamma(N+1) + \varepsilon_{\text{HOMO}}^\gamma(N+1)]^2, \quad (2)$$

where the ionization potential of the neutral species with N electrons, $\text{IP}^\gamma(N)$, is determined from DFT via a Δ SCF approach from total energy differences as $\text{IP}^\gamma(N) = E_{\text{tot}}^\gamma(N-1) - E_{\text{tot}}^\gamma(N)$. Here, $E_{\text{tot}}^\gamma(N)$ and $E_{\text{tot}}^\gamma(N-1)$ are total energies of the neutral and cation species, respectively. This procedure enforces the DFT ionization

potential theorem,^{65,66,69,88} i.e., the energy of the Kohn–Sham highest occupied molecular orbital (HOMO) is equal to the negative of the first ionization potential (IP). For molecules with an unbound $N + 1$ anionic state, only the first of these two terms is minimized, following previous work.⁶³ The hexatriene, benzoquinone, octatetraene, and tetrazine molecules were found to have a bound anionic state within Thiel's set, with all other molecules found to have an unbound anionic state. The optimal parameters obtained within this framework for the molecules studied are given in Fig. 2.

III. RESULTS AND DISCUSSION

A. Ionization potentials from the GW100 set

Here, we investigate the quality of the G_0W_0 @OTRSH ionization potential, or gKS HOMO eigenvalue, against CCSD(T) reference values for the GW100 set.

It is important to first assess the ionization potentials because the G_0W_0 -corrected gKS eigenvalues are a key ingredient in the subsequent BSE step of the calculation. The results of our OTRSH and G_0W_0 @OTRSH calculations for each molecule appear in the supplementary material. In Table I, we summarize the overall performance of each method with the MSE and MAE.

Most of the molecules in the GW100 set do not have a bound $N + 1$ anionic state; therefore, the screening parameter γ was optimized using the first term of Eq. (2) as explained above (IP theorem). The range of γ obtained with this procedure is rather wide due to the variety of chemical species present in the set. For instance, the rare-gas atoms minimize $J^2(\gamma)$ for very large values of γ , the maximum being the helium atom with $\gamma = 0.92 \text{ bohr}^{-1}$.

For G_0W_0 based on OTRSH, we obtain a MSE of 0.04 eV and a MAE of 0.12 eV for the ionization potential (the negative of the HOMO energy). As a comparison, the MAE of G_0W_0 @HF is 0.30 eV.⁷⁸ In Ref. 78, the lowest MAE is 0.15 eV, which is obtained with a global hybrid based on PBE0 with a fixed content of exact exchange, 75%.

As a simplification of OTRSH, we also use an optimization of γ inspired by Atalla *et al.*⁸⁹ Select the γ range-parameter at which the G_0W_0 @OTRSH HOMO energy is equal to the OTRSH HOMO energy. This procedure has the advantage of avoiding the $N - 1$ cationic state calculation. The obtained MAE is similar to the one obtained in the regular approach, 0.12 eV. These are the lowest MAEs in the literature reported so far, and suggest BSE calculations

TABLE I. Mean signed error (MSE) and mean absolute error (MAE) for the ionization potentials of the GW100 set with respect to CCSD(T) reference. The OTRSH parameters have been obtained in two ways: by either imposing the fulfillment of the IP theorem or imposing the equality between the OTRSH and GW HOMO energies.

	MSE (eV)	MAE (eV)
OTRSH (IP theorem)	0.12	0.22
GW@OTRSH (IP theorem)	0.04	0.12
GW@OTRSH (HOMO equality)	0.04	0.12
GW@PBEh (0.75) ^a	0.04	0.15
GW@HF ^a	0.26	0.30

^aReference 78.

on top of G_0W_0 @OTRSH will be accurate, as we now show for the Thiel's set.

B. Neutral excitations from Thiel's set

In what follows, we compare GW-BSE results for OTRSH starting points for a subset of the Thiel's set singlets against wave-function theory-based BTEs of excitation energies, extending recent work⁶³ to include a comprehensive analysis of the OTRSH starting point. As mentioned, these BTEs were obtained with multi-state multi-configurational second-order perturbation theory such as (MS-CASPT2) and various coupled cluster theories, such as coupled cluster with singles, doubles, and perturbative triples (CCSD(T)).⁷⁴ We also consider in our analysis, for comparison, evGW and TDDFT using OTRSH and other functionals.

The optimally tuned γ values reported in Fig. 2 are consistent with those reported for parameter tuning for similar organic molecules in recent literature,^{72,90,99} and match γ values tuned with $\alpha = 0.2$ previously reported for Thiel's set.⁶² The tuned γ values span the range of 0.22–0.36 bohr^{-1} across Thiel's set. Among the unsaturated aliphatic hydrocarbons, γ decreases with increasing chain length. The larger ring structures, cyclopentadiene and norbornadiene, tune to the same γ value while the smaller ring structure, cyclopropene, tunes to a larger value. Among the nucleobases, the single double ring structure among the four ring structures tunes to the smallest γ . Despite structural similarity between thymine and uracil (with the difference of a methyl group), we find that uracil has a larger γ than the γ parameters for thymine and cytosine. Among aromatic hydrocarbons and heterocycles, the pattern of a smaller γ value corresponding to a larger system holds for the one- and two-ring structures, benzene and naphthalene, respectively. The series of single-ring structures with nitrogen substitutions in various locations on the ring do not exhibit a pattern between γ value and the number of nitrogens in the ring.

Clear trends emerge between structure and optimal γ . Decreasing optimal γ with increasing system size is one such pattern, observable with increasing aliphatic hydrocarbon chain length and increasing aromatic ring size. Previous work exploring the relationship between system size and optimal γ value attributed the tuned γ parameter decrease with increasing system size to delocalization error in DFT.^{91,100} However, this observation does not dominate the relationship between γ and molecular structure. Adenine is a two-ring structure with multiple nitrogen substitutions, and it has the same tuned γ as the single-ring pyridazine molecule. This example defies the linear relationship between molecule size and γ . This demonstrates that an explanation for the effect of molecular structure on optimum γ requires further analysis.

Figure 3 reports the mean absolute error (MAE) and the mean signed deviation (MSD) of singlet excitations across molecules in Thiel's set with respect to BTEs for G_0W_0 -BSE and evGW-BSE at multiple starting points, including OTRSH. Functionals are arranged from left to right by increasing amounts of long-range exact exchange. For single-shot G_0W_0 approaches, the MSDs and MAEs reflect a strong starting point dependence, as previously reported.³⁴ As the proportion of long-range exact exchange increases, the MSD evolves from negative (about 1 eV for a PBE starting point, and more than 0.6 eV for PBE0 and B3LYP) to nearly zero for the G_0W_0 -BSE@OTRSH approximation. Use of the TDA

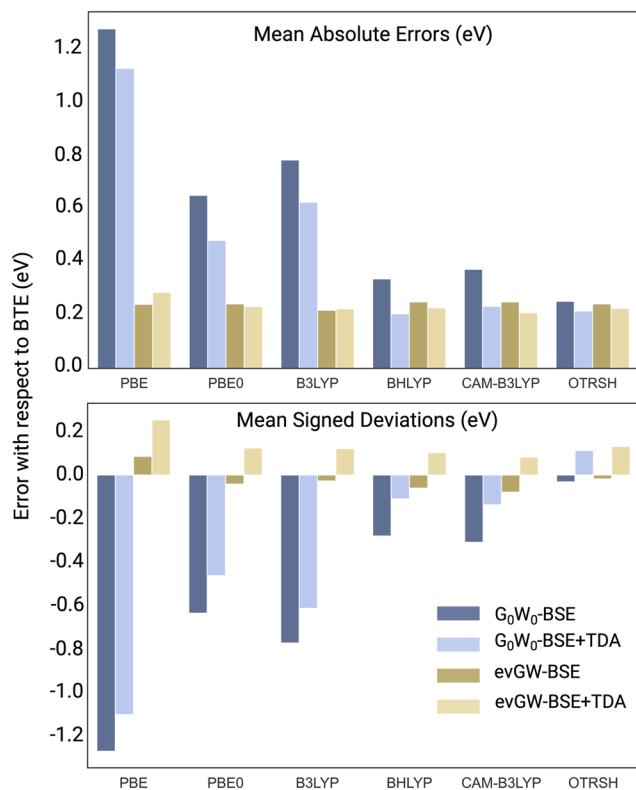


FIG. 3. Summary of MAEs and MSDs for singlets as calculated by G_0W_0 -BSE and evGW-BSE when comparing BTEs from high-level quantum chemistry wavefunction-based methods, including the multireference CASPT2 technique, and coupled cluster theories. The exchange-correlation functionals are displayed, from left to right, in order of increasing fraction of long-range exact exchange. All calculations utilize the aug-cc-pVTZ basis set.

modestly reduces the MAE in the single-shot case for all starting points, although only by about 0.1 eV or less. Notably, eigenvalue self-consistency greatly reduces both the MAE and MSD, largely eliminating the starting point dependence and leading to similar results for all functionals. Every functional compared in this work, perhaps with the exception of OTRSH, yields a disparity in reported MAE and MSD between evGW-BSE and G_0W_0 -BSE.

The trends in Fig. 3 demonstrate that OTRSH is the superior DFT starting point for one-shot calculations among all the approaches considered for the selected molecules belonging to Thiel's set. This optimally tuned functional produced the lowest MSDs and MAEs and exhibited remarkably similar error results between the evGW-BSE and G_0W_0 -BSE approaches. This performance for neutral excitations can be attributed to the OTRSH functional satisfying the IP theorem by system-specific tuning. Thus, eigenvalue self-consistency leads to minimal or negligible improvement.

The distribution of error for G_0W_0 -BSE@OTRSH is centered around zero (supplementary material Fig. S1). This lack of systematic bias in G_0W_0 -BSE@OTRSH calculations is notable particularly

in comparison to the structurally comparable CAM-B3LYP functional, which has a similar distribution of error shifted away from zero. All functionals except for OTRSH tend to underestimate singlets. The PBE starting point is most drastic in this respect, with error concentrated around -1.3 eV. The PBE0 and B3LYP starting points demonstrate similar error concentration around -1 eV, with several outliers in positive error.

While GW-BSE within the TDA has not been extensively studied for small molecules, the TDA has been shown to blue shift excitation energies of azobenzene,⁹² an overestimate attributed to the mixed exciton-plasmon character of neutral excitations in confined systems such as molecules (therefore the need for treatment of the interaction of electron-hole excitations at positive and negative energies). More recent work has shown that the TDA can lead to an improvement in GW-BSE singlet excitation energies in gas-phase acene molecules when using an OTRSH starting point,⁶² ostensibly due to cancellation of errors. Here, consistent with Rangel *et al.* (Ref. 62), for G_0W_0 -BSE, we find that the MSD is improved by the TDA for every starting point except OTRSH (Fig. 3). For evGW-BSE, most starting points' MSDs are worsened by the TDA, including G_0W_0 -BSE@OTRSH.

A comparison between the accuracy of G_0W_0 -BSE@OTRSH and TDDFT@OTRSH is presented in Fig. 4. We see that OTRSH leads to excellent results in comparison to the BTE when used in either formalism; however, G_0W_0 -BSE@OTRSH is superior to TDDFT@OTRSH for Thiel's set. Notably, a divergence in predictive accuracy between G_0W_0 -BSE and TDDFT with respect to the BTE occurs as singlet energies increase. TDDFT@OTRSH performs better for lower energy neutral excitations (<6 eV) than it does for higher-energy neutral excitations. G_0W_0 -BSE@OTRSH does not have this higher-energy error tendency. G_0W_0 -BSE outperforms TDDFT in terms of overall error when combined with OTRSH and BHLYP; however, TDDFT results in less overall error than

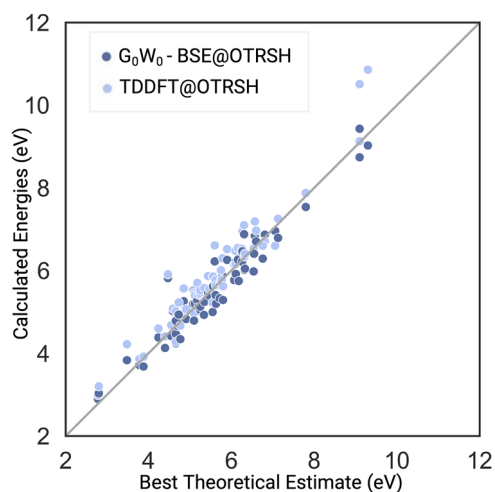


FIG. 4. Comparison of correlation plots for TDDFT and G_0W_0 -BSE predictions for singlet energies as compared to BTE singlet energies. In this comparison, G_0W_0 -BSE has qualitatively superior prediction accuracy to TDDFT, though both methods perform well.

G_0W_0 -BSE when used with PBE, PBE0, B3LYP, or CAM-B3LYP. This trend is further examined in Figs. 5 and 6. The divergence of TDDFT@OTRSH from the BTE seen in Fig. 4 is reflected in larger MAE and MSD for TDDFT@OTRSH than G_0W_0 -BSE. The decreasing error for G_0W_0 -BSE result across functionals suggests G_0W_0 -BSE has more dependence on the starting point than TDDFT.^{34,35} The use of G_0W_0 -BSE with any functional produces an MSD that tends toward negative values. No similar trend in MSD holds for TDDFT. Figure 6 examines the MSD and MAE by splitting all examined singlets into three overlapping subsections: (1) all singlets corresponding to BTE values below 4.0 eV in dataset, (2) all singlets corresponding to BTE values below 6.0 eV in the dataset, and finally (3) all singlets in the examined dataset. This analysis shows that the MAE is energy-dependent for both TDDFT@OTRSH and G_0W_0 -BSE@OTRSH. Through the lens of MSD, G_0W_0 -BSE@OTRSH has far greater accuracy than TDDFT when considering singlets of high and low energies.

Previous studies reporting calculations performed on organic systems have reported TDDFT with OTRSH to overestimate

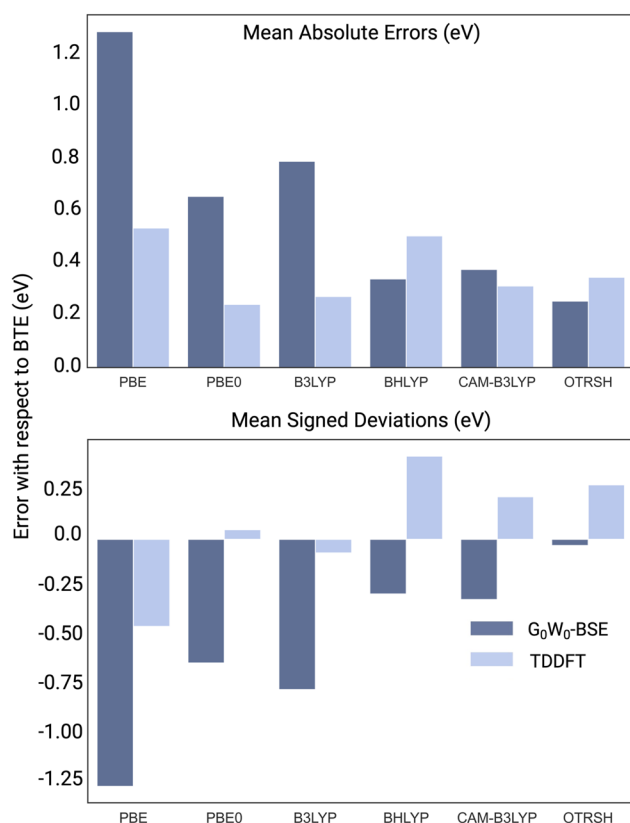


FIG. 5. Summary of MAEs and MSDs of singlets when compared to BTEs from high-level quantum chemistry wavefunction-based methods for both G_0W_0 -BSE and TDDFT approximations. The exchange-correlation functionals are listed in order of increasing HF exact exchange. Error from TDDFT@PBE,⁹³ TDDFT@PBE0,⁹³ TDDFT@BHLYP,⁷⁵ TDDFT@B3LYP,⁷⁵ and TDDFT@CAM-B3LYP⁹³ was sourced from respective citation publications.

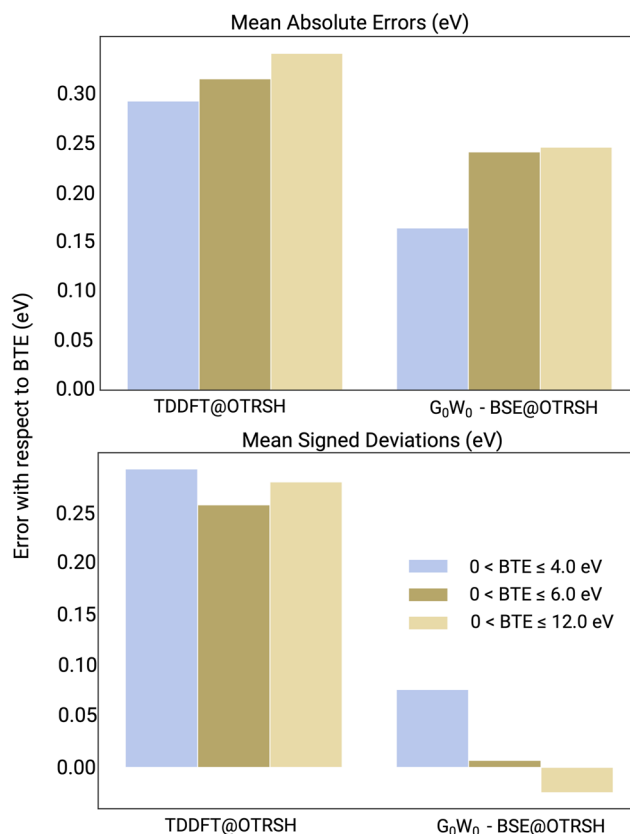


FIG. 6. Breakdown of MAEs and MSDs between TDDFT and G_0W_0 -BSE with the use of the OTRSH functional for singlet excitations. Singlet excitations are analyzed in three categories: The first comprises of all excitations corresponding to a BTE value of below 4.0 eV, the second comprises of all excitations below a BTE value of 6.0 eV, and the third is the entire set of singlets.

excitation energies with respect to GW-BSE.^{76,94} Increasing discrepancy with excitation energy was not captured, however, among calculations on Thiel's set between TDDFT and G_0W_0 -BSE@PBE0, which instead reported error without an energy-dependent trend.⁹⁵ Further investigation into the role of functional and singlet character in excitation energy differences between TDDFT and GW-BSE is warranted.

The strong performance of OTRSH as a starting point for GW-BSE suggests, as has been shown for related approaches such as Koopmans' compliant functionals and localized orbital scaling corrections, that the GW step may be passed in certain cases if accurate quasiparticle energies can be obtained via an alternative route.^{96,97}

IV. CONCLUSIONS

In this work, we have reported a benchmark study on ionization potentials from the GW100 set of small but diverse molecules and on neutral singlet excitations belonging to Thiel's set of small

organic molecules. The neutral excitations have been calculated with both TDDFT and two formulations of GW-BSE: G_0W_0 -BSE and $evGW$ -BSE. Our calculations indicate that OTRSH is a superior starting point for G_0W_0 and for G_0W_0 -BSE and the use of OTRSH minimizes starting point dependence for calculations performed on small molecules. Results obtained from these calculations have appropriate accuracy with respect to higher-order wavefunction-based theories while requiring reduced computational expense. When compared to TDDFT results for the same singlet excitations, G_0W_0 -BSE produces more accurate singlet results, most notably for higher excitation energies. Future studies investigating multicomponent systems and evaluating the OTRSH starting point beyond the gas phase would be of significant interest.

SUPPLEMENTARY MATERIAL

The [supplementary material](#) includes singlet excitations for Thiel's set and a plot correlating the MSD in BSE calculations with the GW HOMO–LUMO gap, as discussed in Sec. III.

ACKNOWLEDGMENTS

This work was supported by the U.S. Department of Energy, Basic Energy Sciences, Chemical Sciences, Geosciences, and Biosciences Division, under Contract No. DE-AC02-05CH11231. We acknowledge the permission granted for the use of computational resources at the National Energy Research Scientific Computing Center (NERSC). This work was also performed using HPC resources from GENCI-CCRT-TGCC (Grants No. 2022-096018). We thank L. Kronik and S. Refaely-Abramson for useful discussions and thank Dr. Dave Small and Dr. Kathleen Durkin and acknowledge the Molecular Graphics and Computation Facility (Grant No. NIH S10OD023532) at the University of California Berkeley for computational resources and assistance with calculations.

AUTHOR DECLARATIONS

Conflict of Interest

The authors have no conflicts to disclose.

Author Contributions

Caroline A. McKeon: Data curation (equal); Formal analysis (equal); Writing – original draft (equal); Writing – review & editing (equal). **Samia M. Hamed:** Formal analysis (equal); Writing – original draft (equal); Writing – review & editing (supporting). **Fabien Bruneval:** Data curation (equal); Formal analysis (equal); Funding acquisition (equal); Writing – original draft (supporting); Writing – review & editing (supporting). **Jeffrey B. Neaton:** Funding acquisition (equal); Investigation (equal); Project administration (equal); Writing – review & editing (equal).

DATA AVAILABILITY

The data that support the findings of this study are available from the corresponding author upon reasonable request.

REFERENCES

- H. Chen, M. Armand, G. Demailly, F. Dolhem, P. Poizot, and J.-M. Tarascon, *ChemSusChem* **1**, 348 (2008).
- K. Sharma, V. Sharma, and S. S. Sharma, *Nanoscale Res. Lett.* **13**, 381 (2018).
- S. Kundu and A. Patra, *Chem. Rev.* **117**, 712 (2017).
- A. D. Laurent and D. Jacquemin, *Int. J. Quantum Chem.* **113**, 2019 (2013).
- X. Blase, I. Duchemin, and D. Jacquemin, *Chem. Soc. Rev.* **47**, 1022 (2018).
- C. Liu, J. Kloppenburg, Y. Yao, X. Ren, H. Appel, Y. Kanai, and V. Blum, *J. Chem. Phys.* **152**, 044105 (2020).
- V. Ziaei and T. Bredow, *J. Phys.: Condens. Matter* **30**, 395501 (2018).
- D. Jacquemin, I. Duchemin, A. Blondel, and X. Blase, *J. Chem. Theory Comput.* **12**, 3969 (2016).
- O. Çaylak and B. Baumeier, *J. Chem. Theory Comput.* **17**, 879 (2021).
- P.-F. Loos, A. Scemama, and D. Jacquemin, *J. Phys. Chem. Lett.* **11**, 2374 (2020).
- C. Suellen, R. G. Freitas, P.-F. Loos, and D. Jacquemin, *J. Chem. Theory Comput.* **15**, 4581 (2019).
- P.-F. Loos, F. Lipparini, M. Boggio-Pasqua, A. Scemama, and D. Jacquemin, *J. Chem. Theory Comput.* **16**, 1711 (2020).
- D. Hait, Y. H. Liang, and M. Head-Gordon, *J. Chem. Phys.* **154**, 074109 (2021).
- E. Runge and E. K. U. Gross, *Phys. Rev. Lett.* **52**, 997 (1984).
- M. A. L. Marques and E. K. U. Gross, *Annu. Rev. Phys. Chem.* **55**, 427 (2004).
- M. E. Casida, *Recent Adv. Density Funct. Methods* **1**, 155 (1995).
- R. Sarkar, M. Boggio-Pasqua, P.-F. Loos, and D. Jacquemin, *J. Chem. Theory Comput.* **17**, 1117 (2021).
- J. Han, D. R. Rehn, T. Buckup, and A. Dreuw, *J. Phys. Chem. A* **124**, 8446 (2020).
- Fundamentals of Time-dependent Density Functional Theory*, edited by M. A. L. Marques, N. T. Maitra, F. M. S. Nogueira, E. K. U. Gross, and A. Rubio (Springer, Berlin, Heidelberg, 2012).
- J. D. Escudero and A. Laurent, *Time-Dependent Density Functional Theory: A Tool to Explore Excited States* (Springer, Cham, 2017).
- S. Corni, S. Pipolo, and R. Cammi, *J. Phys. Chem. A* **119**, 5405 (2015).
- A. Nakata, T. Tsuneda, and K. Hirao, *J. Chem. Phys.* **135**, 224106 (2011).
- D. J. Tozer and N. C. Handy, *J. Chem. Phys.* **109**, 10180 (1998).
- B. Le Guennic and D. Jacquemin, *Acc. Chem. Res.* **48**, 530 (2015).
- A. Prlj, B. F. E. Curchod, A. Fabrizio, L. Floryan, and C. Corminboeuf, *J. Phys. Chem. Lett.* **6**(1), 13 (2015).
- A. Dreuw and M. Head-Gordon, *J. Am. Chem. Soc.* **126**, 4007 (2004).
- S. Kümmel, *Adv. Energy Mater.* **7**, 1700440 (2017).
- T. Stein, L. Kronik, and R. Baer, *J. Am. Chem. Soc.* **131**, 2818 (2009).
- M. J. G. Peach and D. J. Tozer, *J. Phys. Chem. A* **116**, 9783 (2012).
- S. Hirata and M. Head-Gordon, *Chem. Phys. Lett.* **314**, 291 (1999).
- A. Fetter and J. Walecka, *Quantum Theory of Many-Particle Systems* (MacGraw-Hill, New York, NY, 1971).
- G. Mahan, *Many-Particle Physics* (Kluwer Academic/Plenum Publishers, 2000).
- A. Szabo and N. Ostlund, *Modern Quantum Chemistry: Introduction to Advanced Electronic Structure Theory* (Dover Publications, Mineola, NY, 1996).
- F. Bruneval, S. M. Hamed, and J. B. Neaton, *J. Chem. Phys.* **142**, 244101 (2015).
- D. Jacquemin, I. Duchemin, and X. Blase, *J. Chem. Theory Comput.* **11**, 3290 (2015).
- C. Holzer and W. Klopper, *J. Chem. Phys.* **150**, 204116 (2019).
- G. Tirimbò, V. Sundaram, O. Çaylak, W. Scharpach, J. Sijen, C. Junghans, J. Brown, F. Z. Ruiz, N. Renaud, J. Wehner, and B. Baumeier, *J. Chem. Phys.* **152**, 114103 (2020).
- L. Kronik and J. B. Neaton, *Annu. Rev. Phys. Chem.* **67**, 587 (2016).
- X. Blase, I. Duchemin, D. Jacquemin, and P.-F. Loos, *J. Phys. Chem. Lett.* **11**, 7371 (2020).
- M. J. van Setten, F. Caruso, S. Sharifzadeh, X. Ren, M. Scheffler, F. Liu, J. Lischner, L. Lin, J. R. Deslippe, S. G. Louie, C. Yang, F. Weigend, J. B. Neaton, F. Evers, and P. Rinke, *J. Chem. Theory Comput.* **11**, 5665 (2015).

- ⁴¹F. Bruneval, T. Rangel, S. M. Hamed, M. Shao, C. Yang, and J. B. Neaton, *Comput. Phys. Commun.* **208**, 149 (2016).
- ⁴²G. Strinati, *Riv. Nuovo Cimento* **11**, 1–86 (1988).
- ⁴³F. Aryasetiawan and O. Gunnarsson, *Rep. Prog. Phys.* **61**, 237 (1998).
- ⁴⁴G. Onida, L. Reining, and A. Rubio, *Rev. Mod. Phys.* **74**, 601 (2002).
- ⁴⁵S. Albrecht, L. Reining, R. Del Sole, and G. Onida, *Phys. Rev. Lett.* **80**, 4510 (1998).
- ⁴⁶E. L. Shirley, *Phys. Rev. Lett.* **80**, 794 (1998).
- ⁴⁷M. Rohlfing and S. G. Louie, *Phys. Rev. Lett.* **81**, 2312–2315 (1998).
- ⁴⁸T. Körzdörfer and N. Marom, *Phys. Rev. B: Condens. Matter Mater. Phys.* **86**, 041110 (2012).
- ⁴⁹N. Marom, *J. Phys.: Condens. Matter* **29**, 103003 (2017).
- ⁵⁰F. Bruneval and M. A. L. Marques, *J. Chem. Theory Comput.* **9**, 324 (2013).
- ⁵¹D. Jacquemin, E. A. Perpète, G. E. Scuseria, I. Ciofini, and C. Adamo, *J. Chem. Theory Comput.* **4**, 123 (2008).
- ⁵²M. J. G. Peach, P. Benfield, T. Helgaker, and D. J. Tozer, *J. Chem. Phys.* **128**, 044118 (2008).
- ⁵³K. A. Nguyen, P. N. Day, and R. Pachter, *Int. J. Quantum Chem.* **110**, 2247 (2010).
- ⁵⁴T. Yanai, D. P. Tew, and N. C. Handy, *Chem. Phys. Lett.* **393**, 51–57 (2004).
- ⁵⁵S. Refaely-Abramson, S. Sharifzadeh, N. Govind, J. Autschbach, J. B. Neaton, R. Baer, and L. Kronik, *Phys. Rev. Lett.* **109**, 226405 (2012).
- ⁵⁶D. A. Egger, S. Weissman, S. Refaely-Abramson, S. Sharifzadeh, M. Dauth, R. Baer, S. Kümmel, J. B. Neaton, E. Zojer, and L. Kronik, *J. Chem. Theory Comput.* **10**, 1934 (2014).
- ⁵⁷L. Gallandi and T. Körzdörfer, *J. Chem. Theory Comput.* **11**, 5391 (2015).
- ⁵⁸L. Gallandi, N. Marom, P. Rinke, and T. Körzdörfer, *J. Chem. Theory Comput.* **12**, 605 (2016).
- ⁵⁹J. W. Knight, X. Wang, L. Gallandi, O. Dolgouitcheva, X. Ren, J. V. Ortiz, P. Rinke, T. Körzdörfer, and N. Marom, *J. Chem. Theory Comput.* **12**, 615 (2016).
- ⁶⁰J. Bois and T. Körzdörfer, *J. Chem. Theory Comput.* **13**, 4962 (2017).
- ⁶¹M. Kumar, J. Provazza, and D. F. Coker, *J. Chem. Phys.* **154**, 224109 (2021).
- ⁶²T. Rangel, S. M. Hamed, F. Bruneval, and J. B. Neaton, *J. Chem. Phys.* **146**, 194108 (2017).
- ⁶³T. Rangel, S. M. Hamed, F. Bruneval, and J. B. Neaton, *J. Chem. Theory Comput.* **12**, 2834 (2016).
- ⁶⁴T. Leininger, H. Stoll, H.-J. Werner, and A. Savin, *Chem. Phys. Lett.* **275**, 151 (1997).
- ⁶⁵J. P. Perdew, R. G. Parr, M. Levy, and J. L. Balduz, *Phys. Rev. Lett.* **49**, 1691 (1982).
- ⁶⁶U. Salzner and R. Baer, *J. Chem. Phys.* **131**, 231101 (2009).
- ⁶⁷M. Levy, J. P. Perdew, and V. Sahni, *Phys. Rev. A* **30**, 2745 (1984).
- ⁶⁸J. P. Perdew and M. Levy, *Phys. Rev. B: Condens. Matter Mater. Phys.* **56**, 16021 (1997).
- ⁶⁹C.-O. Almbladh and U. von Barth, *Phys. Rev. B: Condens. Matter Mater. Phys.* **31**, 3231 (1985).
- ⁷⁰R. Baer and D. Neuhauser, *Phys. Rev. Lett.* **94**, 043002 (2005).
- ⁷¹E. Livshits and R. Baer, *Phys. Chem. Chem. Phys.* **9**, 2932 (2007).
- ⁷²L. Kronik, T. Stein, S. Refaely-Abramson, and R. Baer, *J. Chem. Theory Comput.* **8**, 1515 (2012).
- ⁷³S. Refaely-Abramson, S. Sharifzadeh, M. Jain, R. Baer, J. B. Neaton, and L. Kronik, *Phys. Rev. B: Condens. Matter Mater. Phys.* **88**, 081204 (2013).
- ⁷⁴M. Schreiber, M. R. Silva-Junior, S. P. A. Sauer, and W. Thiel, *J. Chem. Phys.* **128**, 134110 (2008).
- ⁷⁵M. R. Silva-Junior, M. Schreiber, S. P. A. Sauer, and W. Thiel, *J. Chem. Phys.* **133**, 174318 (2010).
- ⁷⁶Z. Hashemi and L. Leppert, *J. Phys. Chem. A* **125**, 2163 (2021).
- ⁷⁷K. Krause, M. E. Harding, and W. Klopper, *Mol. Phys.* **113**, 1952 (2015).
- ⁷⁸F. Bruneval, N. Dattani, and M. J. van Setten, *Front. Chem.* **9**, 749779 (2021).
- ⁷⁹P. J. Stephens, F. J. Devlin, C. F. Chabalowski, and M. J. Frisch, *J. Phys. Chem.* **98**, 11623 (1994).
- ⁸⁰X. Blase, C. Attaccalite, and V. Olevano, *Phys. Rev. B: Condens. Matter Mater. Phys.* **83**, 115103 (2011).
- ⁸¹M. Shishkin, M. Marsman, and G. Kresse, *Phys. Rev. Lett.* **99**, 246403 (2007).
- ⁸²G. P. Chen, V. K. Voora, M. M. Agee, S. G. Balasubramani, and F. Furche, *Annu. Rev. Phys. Chem.* **68**, 421 (2017).
- ⁸³T. H. Dunning, *J. Chem. Phys.* **90**, 1007 (1989).
- ⁸⁴O. Vahtras, J. Almlöf, and M. W. Feyereisen, *Chem. Phys. Lett.* **213**, 514–518 (1993).
- ⁸⁵F. Weigend and R. Ahlrichs, *Phys. Chem. Chem. Phys.* **7**, 3297 (2005).
- ⁸⁶M. Srebro and J. Autschbach, *J. Phys. Chem. Lett.* **3**, 576 (2012).
- ⁸⁷M. A. Rohrdanz, K. M. Martins, and J. M. Herbert, *J. Chem. Phys.* **130**, 054112 (2009).
- ⁸⁸A. J. Cohen, P. Mori-Sánchez, and W. Yang, *Phys. Rev. B: Condens. Matter Mater. Phys.* **77**, 115123 (2008).
- ⁸⁹V. Atalla, M. Yoon, F. Caruso, P. Rinke, and M. Scheffler, *Phys. Rev. B* **88**, 165122 (2013).
- ⁹⁰S. Bhandari and B. D. Dunietz, *J. Chem. Theory Comput.* **15**, 4305 (2019).
- ⁹¹K. Garrett, X. Sosa Vazquez, S. B. Egri, J. Wilmer, L. E. Johnson, B. H. Robinson, and C. M. Isborn, *J. Chem. Theory Comput.* **10**, 3821 (2014).
- ⁹²M. Grüning, A. Marini, and X. Gonze, *Nano Lett.* **9**, 2820 (2009).
- ⁹³D. Jacquemin, V. Wathelet, E. A. Perpète, and C. Adamo, *J. Chem. Theory Comput.* **5**, 2420 (2009).
- ⁹⁴T. B. de Queiroz, E. R. de Figueroa, M. D. Coutinho-Neto, C. D. Maciel, E. Tapavicza, Z. Hashemi, and L. Leppert, *J. Chem. Phys.* **154**, 044106 (2021).
- ⁹⁵X. Gui, C. Holzer, and W. Klopper, *J. Chem. Theory Comput.* **14**, 2127 (2018).
- ⁹⁶N. Colonna, N. L. Nguyen, A. Ferretti, and N. Marzari, *J. Chem. Theory Comput.* **15**, 1905 (2019).
- ⁹⁷J. Li, Y. Jin, N. Q. Su, and W. Yang, *J. Chem. Phys.* **156**, 154101 (2022).
- ⁹⁸L. Hedin and S. Lundqvist, in *Solid State Physics*, Vol. 23, edited by F. Seitz, D. Turnbull, and H. Ehrenreich (Academic Press, 1970) pp. 1–181.
- ⁹⁹S. Refaely-Abramson, R. Baer, and L. Kronik, *Phys. Rev. B Condens. Matter* **84**, 075144 (2011).
- ¹⁰⁰P. Mori-Sánchez, A. J. Cohen, and W. Yang, *Phys. Rev. Lett.* **100**, 146401 (2008).